

dependent population controls for 400 generations. Adaptation occurred, as shown by the superiority of adapted strains over nonadapted parental strains. And finally, K-selected strains are superior under both density-dependent and independent population controls. Thus, no trade-off in adaptation to r and K selection occurred here.

In the hypothesis, predicted life history features are determined solely by the density-dependent or independent status of controlling factors. These experiments are valid then, to the extent that they accurately simulate population controls.

The growth of experimental populations under density-independent control closely fits the circumstances for r selection (1). Populations under density-dependent control did undergo a brief initial period of unlimited growth but most of the growth occurred under strong density-dependent limitation. Therefore, although selection under this regime may not be perfect, it is predominantly density-dependent and clearly qualifies as K selection.

Many other questions may be raised in relation to specific genetic mechanisms involved in adaptation in this system. In particular, how do the differences between the types of selection applied ac-

count for the differences observed in adaptive mutants? Answers to this question and others are necessary to a complete understanding of this system.

LEO S. LUCKINBILL

Department of Biology,
Wayne State University,
Detroit, Michigan 48202

References and Notes

1. R. H. MacArthur and E. O. Wilson, *The Theory of Island Biogeography* (Princeton Monographs, Princeton, N.J., 1967); R. H. MacArthur, *Geographic Ecology* (Harper & Row, New York, 1972); E. R. Pianka, *Am. Nat.* **104**, 592 (1970); *ibid.* **106**, 581 (1972).
2. M. L. Cody, *Evolution* **20**, 174 (1966); in *Avian Biology*, D. H. Farner and J. R. King, Eds. (Academic Press, New York, 1970), vol. 1, p. 461; W. G. Abrahamson and M. Gadgil, *Am. Nat.* **107**, 651 (1973); W. G. Abrahamson, *Ecology* **56**, 721 (1975); M. Ganes, K. Vogt, J. Hamrick, J. Calwell, *Am. Nat.* **108**, 880 (1974); S. J. McNaughton, *ibid.* **109**, 251 (1975); W. K. Derickson, *Ecology* **57**, 445 (1976).
3. F. E. Smith, *Ecology* **42**, 403 (1961); D. A. Maelzer, *ibid.* **51**, 810 (1970); R. F. Morris, *Mem. Entomol. Soc. Can.* **31**, 116 (1963); W. W. Murdoch, *Ecology* **51**, 497 (1970); J. L. S. St. Amant, *ibid.*, p. 823.
4. H. M. Wilbur, D. W. Tinkle, J. P. Collins, *Am. Nat.* **108**, 805 (1974).
5. K. C. Atwood, L. K. Schneider, F. J. Ryan, *Cold Spring Harbor Symp. Quant. Biol.* **16**, 345 (1951); F. S. Ryan and L. K. Wainwright, *J. Gen. Microbiol.* **11**, 364 (1954); L. D. Schneider, *Biol. Bull. (Woods Hole, Mass.)* **99**, 331 (1950).
6. R. S. Ryan and L. K. Schneider, *J. Bacteriol.* **56**, 699 (1948); *ibid.* **58**, 181 (1948); *ibid.*, p. 201; *Genetics* **34**, 72 (1940).
7. I thank A. W. Siegel, W. E. Moore, and D. C. Freeman for readings and critical discussion of earlier drafts. Supported by NSF grants BMS75-05368 and DEB77-25600.

24 April 1978; revised 21 August 1978

Calcium Entry Leads to Inactivation of Calcium Channel in *Paramecium*

Abstract. Under depolarizing voltage clamp of *Paramecium* an inward calcium current developed and subsequently relaxed within 10 milliseconds. The relaxation was substantially slowed when most of the extracellular calcium was replaced by either strontium or barium. Evidence is presented that the relaxation is not accounted for by a drop in electromotive force acting on calcium, or by activation of a delayed potassium current. Relaxation of the current must, therefore, result from an inactivation of the calcium channel. This inactivation persisted after a pulse, as manifested by a reduced calcium current during subsequent depolarization. Inactivation was retarded by procedures that reduce net entry of calcium, and was independent of membrane potential. The calcium channel undergoes inactivation as a consequence of calcium entry during depolarization. In this respect, inactivation of the calcium channel departs qualitatively from the behavior described in the Hodgkin-Huxley model of the sodium channel.

The calcium ion performs several important functions in the ciliate *Paramecium* (1-3). Calcium carries the inward current during electrical excitation (2-5) through channels in the surface membrane covering the cilia (6, 7). Within the cilium, the Ca ion activates a re-orientation of axonemal movement, causing the cilia to beat vigorously in reverse (8). Step depolarizations under voltage clamp are accompanied by characteristic membrane currents—an initial

inward current, carried by Ca²⁺ (5, 9), which quickly relaxes (that is, decays) and is followed under moderate and large depolarizing pulses by a delayed outward current attributed to an efflux of K⁺. Relaxation of the initial inward current resembles, superficially, the inactivation (the state of insensitivity to depolarization) exhibited by the early current carried through the Na channels of nerve (10), which inactivate with time as a function of membrane voltage.

Relaxation of the transient inward current in *Paramecium* (5, 9) might result from (i) the development of an outward current that masks a noninactivating steady Ca current, (ii) a drop in the Ca equilibrium potential (E_{Ca}) produced by the entry and intraciliary accumulation of Ca, or (iii) inactivation of the Ca channel. We now provide evidence that inactivation is the major factor causal to the relaxation of the Ca current. More significant, we provide evidence that the inactivation of the Ca system of *Paramecium* does not occur as a direct result of membrane depolarization, but that it occurs as a consequence of Ca entry that follows activation of the Ca channels by depolarization.

Specimens of *P. caudatum* were impaled with current passing and recording electrodes (10 to 30 megohms) for voltage clamping. The membrane was voltage-clamped at a holding potential equal to the resting potential. The recorded resting potential in *Paramecium* is non-specifically sensitive to changes in both monovalent and divalent cation concentration (11). As compared to the behavior typical of metazoan membranes (that is, squid axon) the current-voltage relations for the early inward and late outward currents in *Paramecium* characteristically shift in an amount approximating the change in the resting potential when the extracellular ionic strength is altered. Therefore, when varying extracellular Ca, Ba, and Sr concentrations, potentials were plotted (Figs. 1-3) as displacement from the holding (resting) potential rather than by the more conventional manner of plotting absolute potential. To minimize series resistance errors in the solutions of low ionic strength, an extracellular electrode (10 to 30 megohms) was placed near the cell surface. Membrane voltage steps were 90 percent complete within 1.0 msec, and the capacitive current transients were over within 1.5 msec. Specimens were bathed in a control solution of 1 mM CaCl₂, 4 mM KCl, and 1 mM Hepes (*N*-2-hydroxyethylpiperazine-*N'*-2-ethanesulfonic acid) buffer at pH 7.1. For certain experiments, the 1 mM CaCl₂ was replaced by 0.1 mM CaCl₂ plus 5 mM BaCl₂ or 0.1 mM CaCl₂ plus 5 mM SrCl₂. Some extracellular Ca is required for membrane integrity in *Paramecium*. In another experiment, a mixture of 50 mM CsCl plus 50 mM TEA-Cl (tetraethylammonium-chloride) + 10 mM Pipes [piperazine-*N*-*N'*-bis(2-ethanesulfonic acid)] buffer (pH 7.0) was introduced by iontophoresis into clamped cells, with 10⁻⁹-A, 60-second current pulses.

Depolarization of 5 mV or more in

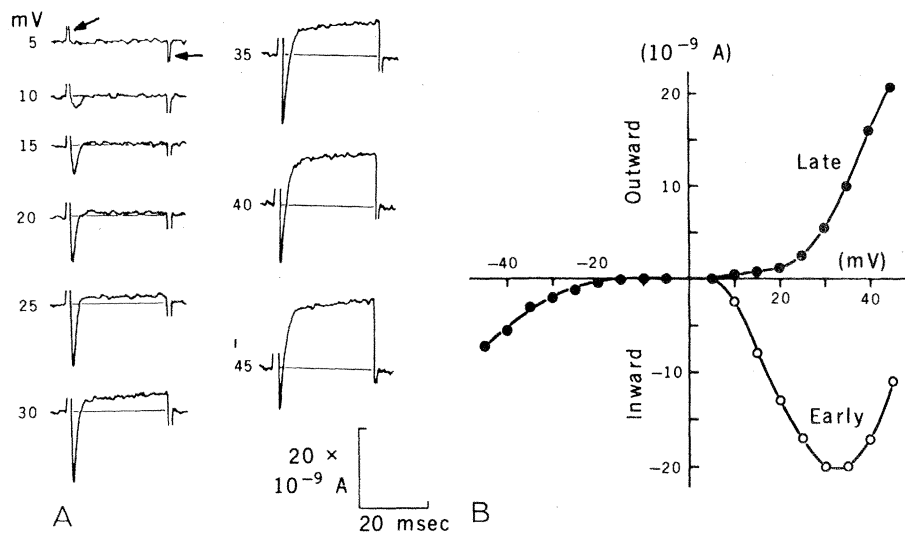


Fig. 1. (A) Membrane currents from a *P. caudatum* cell in 1 mM Ca plus 4 mM K plus 1 mM Hepes buffer solution, pH 7.2, stepped to various potentials from holding potential (-40 mV) with a 30-msec voltage clamp pulse (21°C). Rapid capacitive transients were slowed by limited frequency response of the strip chart recorder. These were partially blocked out for clarity. The number to the left of each trace indicates the amplitude of the pulse. Capacitive artifacts are indicated by arrows in the 5-mV step. (B) Current-voltage relations plotted from data in (A). Open circles represent peak inward current. Closed circles indicate current measured at the end of the 30-msec pulse. The origin is at the holding potential, which was set to equal the resting potential (V_{rest}) (-40 mV).

control solution produced an inward current transient (downward deflection) after the initial capacitive transient (upward deflection) (Fig. 1A). Steps of from +5 mV to +20 mV generally resulted in a relaxation of the inward current back to approximate zero level during maintained depolarization (Fig. 1A). With depolarizations exceeding 25 mV or 30 mV (where maximum net inward current was observed), the inward current was followed by development of a late outward current (Fig. 1, A and B).

The possibility must be considered that the trajectory of inward current relaxation is generated by development of an outward K current that obscures a noninactivating inward Ca current. The possibility of such a large late outward current offsetting the inward Ca current so as to produce an approximately zero net late current during depolarizations of up to 20 mV was tested by injecting a Cs-TEA mixture to interfere with outward potassium currents. For depolarizations of 30 mV or greater, the Cs-TEA mixture almost completely eliminated the large late outward current (Fig. 2). This is consistent with the reputed K-blocking effectiveness of TEA and Cs ions (12). At depolarizations (5 to 20 mV) that evoke little net outward current, the net inward current relaxed at the same rate as before the injection of the K-blocking agents. The amplitude of the transient Ca current during pulses of this amplitude was also unaffected (or very slightly de-

creased) by the injected Cs plus TEA (Fig. 2). At higher potentials (> 20 mV), the outward current must overlap to some extent with the inward current, for injection of the K-blocking agents does produce a slight slowing of relaxation and a small increase in amplitude of the

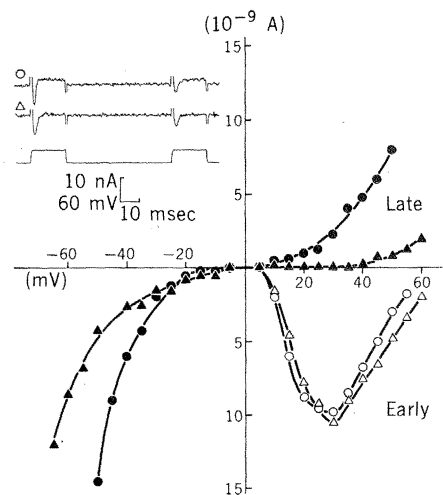


Fig. 2. Current-voltage relations in a cell before (O) and after (Δ) a 5-minute, 10^{-9} -A injection of a mixture containing 50 mM TEA plus 50 mM Cs plus 10 mM Pipes buffer (pH 7.0). The peak inward current (O, Δ) and late outward current (●, ▲) measured at 30 msec from the onset of the pulse were plotted. Origin is the resting potential (V_{rest}), which was -48 mV in both cases. (Inset) Membrane currents recorded before (O) and after (Δ) injection. The paired pulses were both 20-msec, 30-mV steps, separated by a 60-msec interval. The lower trace is the membrane potential.

inward current transient. We conclude then that decay of the inward current represents primarily a relaxation of the Ca current, and not merely the activation of an outward K current that sums algebraically with a noninactivating Ca current.

Two lines of evidence rule out the possibility that it is merely a drop in E_{Ca} during Ca entry that causes relaxation of the Ca current. (i) Replacement of most of the extracellular Ca by an equal amount of Ba or Sr resulted in a significantly slowed relaxation of inward current (Fig. 3A). Both Ba and Sr carry peak currents similar in amplitude to Ca, and so carry similar or greater numbers of the respective cations into the cell by the time of peak inward current (which is somewhat delayed in Sr or Ba relative to the time of peak current in Ca). These cations, therefore, must experience a reduction in driving force similar or greater to that of Ca as these ions enter and accumulate. (ii) The approximate reduction in E_{Ca} during an inward Ca current can be calculated directly. The inward current trace (Fig. 3B) was integrated to peak current, which corresponds to a total cellular entry of 5.7×10^{-15} mole of Ca. This current enters exclusively through the region of membrane covering the cilia (6, 7). Since each cell has about 1.5×10^4 cilia (7), and each cilium has a volume of $6 \mu\text{m}^3$, the Ca^{2+} entering between onset and peak of the inward current, if evenly distributed in the cilium, will reach a concentration of $1.2 \times 10^{-5}M$. This figure agrees well with previous calculations (2, 5). With 5 mM extracellular Ca, the driving force acting on Ca at the peak of the inward current will therefore be 76 mV. Integrating the remaining time course of inward current and doubling that figure to compensate for any simultaneous outward K current at that potential (Fig. 2) yields a final Ca concentration of $4 \times 10^{-5}M$ after decay of the inward current. At this concentration, the driving force should be 61 mV, which means a reduction in electromotive force (emf) of only 20 percent relative to the emf present at the peak of the inward current. Passive or active removal (or both) of Ca^{2+} from the ciliary cytosol should, in fact, result in an overestimation of the rise in intraciliary Ca concentration, so that the emf acting on Ca probably drops less than calculated. While there is a significant rise in intraciliary Ca concentration during Ca entry, the attending reduction in E_{Ca} cannot account for the relaxation of the inward current. By process of elimination, then, we conclude that the

relaxation of inward current results from a true inactivation of the Ca channel.

Inactivation of the inward current was examined with paired 20-msec pulses separated by a 60-msec interval. The inactivation persists after the first pulse and is seen during the second pulse as a decrease in the peak inward current (Fig. 3, A and C). The validity of the paired-pulse method for examining Ca inactivation without contamination by changes in K current kinetics was tested by comparing inactivation before and after Cs-TEA injection (Fig. 2, inset), which was done to block outward K currents (12). After Cs-TEA injections that blocked most of the late outward current, the amount of inactivation (that is, pulse II current relative to pulse I current) remained virtually unchanged after injection of the K-blocking agents (Fig. 2, inset). It is unlikely that the reduction in peak inward current during pulse II results from changes in outward K current, for this would require a facilitating K conductance that is both similar in time course to the early inward current,

and insensitive to injected Cs and TEA.

The inactivation of the pulse II current depends on the amplitude of pulse I. In Ca solution, the inward current measured during a fixed-amplitude pulse II exhibited progressively greater inactivation as pulse I approached an amplitude of 60 mV (Fig. 3, A and C). With further increase in pulse I amplitude, however, inactivation, as detected by reduction of the pulse II current, became progressively smaller. The strongly curtailed inactivation associated with pulse I potentials approaching the calculated E_{Ca} (about +120 mV with 1 mM extracellular Ca) suggests that entry of Ca is required for channel inactivation.

Substitution of most of the extracellular Ca with Ba resulted in a profound reduction of the inactivation as measured by the paired-pulse method. Substitution with Sr resulted in an inactivation which was intermediate between inactivations measured in Ca or Ba solutions (Fig. 3, A and C). Both Ba and Sr carry currents presumably through the Ca channel, but their entry

appears to be less effective than Ca entry in producing inactivation of the Ca channel. Since some extracellular Ca was provided to prevent cell lysis, the residual inactivation in Ba solution may have resulted from a small amount of Ca entering along with the Ba. The intermediate inactivation in Sr solution during a single pulse (Fig. 3A) and during paired pulses (Fig. 3C) might be due to either a weak Ca-like action of Sr promoting channel inactivation, or to a larger proportion of Ca entering with Sr than enters with Ba.

If the entry of Ca alone, rather than depolarization, is sufficient to produce inactivation of the Ca channel, prolonged depolarization without Ca entry should not be accompanied by inactivation. This was tested as follows. A 30-mV test depolarization was presented to elicit an inward current (to serve as a control). This pulse was then preceded, without interval, by a variable-amplitude 100-msec conditioning step (Fig. 3D). A 5 mM Sr plus 0.1 mM Ca solution was used to prolong the inward current be-

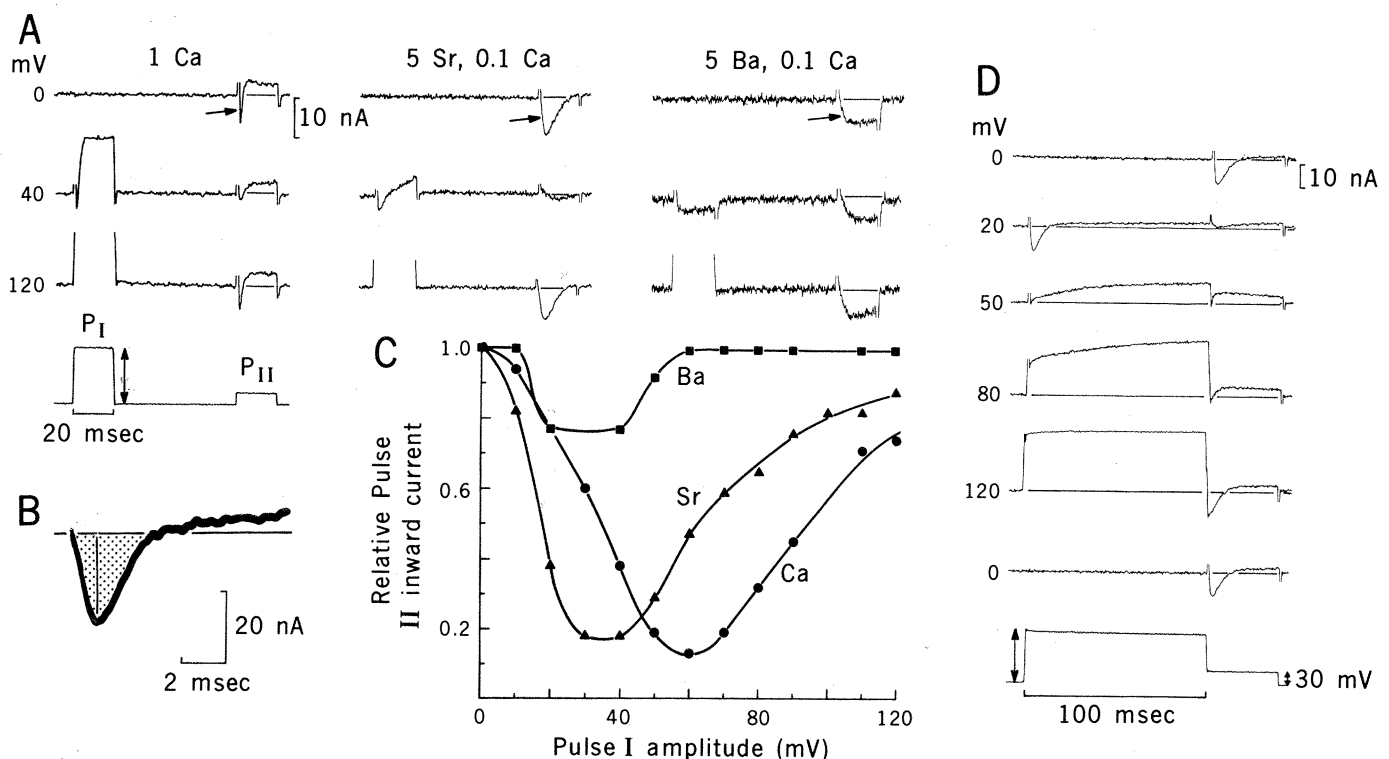


Fig. 3. Inactivation of the inward current. (A) Membrane currents in 1 mM Ca, 5 mM Sr plus 0.1 mM Ca, and 5 mM Ba plus 0.1 mM Ca. Each solution also contained 4 mM K plus 1 mM Hepes. Representative recordings are shown from three different cells, one in each solution. Pulse I amplitudes are indicated to left. Pulse II was fixed at 20 mV in a Sr and Ba cell, and at 25 mV in a Ca cell. A representative voltage trace is shown at the bottom. The arrows point to inward currents. Initial upward and terminal downward deflections are the capacitive artifacts. (B) Time course of inward current transient during 25-mV voltage step, used for the calculation of the charge entry. The solution consisted of 5 mM Ca plus 4 mM K plus 1 mM Hepes. The stippling shows the current-time integral to peak, and from peak to zero. The small late outward current is activated at this voltage. (C) The relative strength of the pulse II inward current is plotted as a function of the amplitude of the conditioning pulse (I) as in experiment in (A). The ordinate is the ratio of the P_{II} peak current relative to the control current recorded in the absence of P_I . (D) Membrane currents from a cell in a solution of 5 mM Sr, 0.1 mM Ca, 4 mM K, and 1 mM Hepes clamped with a 100-msec variable-amplitude conditioning step followed without interval by a 40-msec, 30-mV test pulse. The conditioning step amplitudes are indicated at the left. Membrane currents without the conditioning pulse are shown before (top trace) and after (bottom trace) the series. Inactivation of the inward tail current is observed after 20-, 50-, and 80-mV steps. Tail currents after the 120-mV conditioning step show no inactivation.

yond any capacitive artifacts, allowing more accurate measurement. The peak inward current during the 30-mV test pulse was small after conditioning steps of low or moderate (20-, 50-, and 80-mV) voltages, indicating partial inactivation during those conditioning steps. However, the current approached the amplitude of the control current after conditioning steps of sufficient positive potential (for example, 120 mV) to retard the entry of Ca and Sr. The absence of inactivation of the inward current after large positive potentials lasting 100 msec indicates that inactivation of the Ca channel does not occur in response to depolarization. Potential-independent inactivation as displayed by the Ca channel departs qualitatively from the potential-dependent inactivation characteristic of the Na channel described in the Hodgkin-Huxley model (10).

The injection of the Ca chelating agent EGTA into *Paramecium* produces prolonged action potentials (13). In voltage clamp experiments we found that injection of EGTA retards inactivation of the Ca current so that relaxation of the early current is slowed, and a net inward current persists for hundreds of milliseconds. This suggests that it is the accumulation of free Ca²⁺ rather than the passage of Ca through its channel that leads to inactivation of the channel.

A possible blocking effect of intracellular Ca²⁺ on the Ca conductance was first indicated in a study of internally perfused barnacle muscle (14). A reduction of the Ca spike after elevation of intracellular EDTA-buffered Ca could not be compensated by a proportional increase in extracellular Ca. Studies on perfused molluscan neuron (15) and tunicate egg (16) also indicate that the Ca conductance can be influenced by EGTA-buffered intracellular Ca concentration. Our study on *Paramecium* indicates that entering Ca²⁺ produces physiological inactivation of the channel, and does so within a time frame suitable to act during the course of a single Ca response (that is, graded Ca action potential of *Paramecium*), and may therefore participate in the repolarization of the excited membrane.

The discovery of this new regulatory activity of the Ca ion has provided a clearer understanding of how Ca entry and accumulation may be regulated in *Paramecium*. Depolarization activates Ca channels, allowing Ca entry through the surface membrane covering the cilia. The rapid rise in Ca concentration in the minute intraciliary space results in a rapid inactivation of the Ca channels, seen as a relaxation of the inward current.

However, complete inactivation under prolonged depolarization is not predicted by our findings, since a steady state must be established between Ca entry and elevation of the intraciliary Ca concentration on the one hand, and the resulting inactivation of Ca channels by elevated intraciliary Ca on the other hand. This negative feedback relation between Ca entry and Ca-dependent inactivation should result, during steady depolarization, in an elevated intraciliary Ca concentration maintained by a small steady Ca current equal to the loss of Ca from the cilium. That a sustained depolarization produces a sustained Ca current and a maintained increment in intraciliary Ca concentration has, in fact, been inferred from the behavior of the cilia under depolarization (17); reversed beating, which relaxes only slowly during prolonged depolarization, is a sensitive indicator of elevated intraciliary Ca concentration (8).

A parallel investigation, by techniques that differ in part from the ones that we used, has also indicated a Ca-dependent, voltage-insensitive inactivation of the Ca conductance in molluscan giant neurons (18). The presence of similar behavior in Ca systems in such phylogenetically diverse organisms suggests that Ca-dependent inactivation may be a universal characteristic of Ca channels.

PAUL BREHM, ROGER ECKERT
Department of Biology and
Ahmanson Laboratory of Neurobiology,
Brain Research Institute, University of
California, Los Angeles 90024

References and Notes

1. Y. Naitoh and R. Eckert, *Science* **164**, 963 (1969).
2. R. Eckert, *ibid.* **176**, 473 (1972).
3. Y. Naitoh, R. Eckert, K. Friedman, *J. Exp. Biol.* **56**, 667 (1972).
4. R. Eckert, Y. Naitoh, H. Machemer, in *Calcium in Biological Systems*, C. J. Duncan, Ed. (Cambridge Univ. Press, Cambridge, 1976); Y. Naitoh and R. Eckert, *Z. Vgl. Physiol.* **61**, 453 (1968); C. Kung and R. Eckert, *Proc. Natl. Acad. Sci. U.S.A.* **69**, 93 (1972).
5. D. Oertel, S. Schein, C. Kung, *Nature (London)* **268**, 120 (1977).
6. K. Dunlap, *J. Physiol. (London)* **271**, 119 (1977).
7. ———, thesis, University of California, Los Angeles (1977).
8. Y. Naitoh and H. Kaneko, *Science* **176**, 523 (1972); R. Eckert and H. Machemer, in *Symposium of the Society for General Physiology*, R. Stephens and S. Inoue, Eds. (Raven, New York, 1975), p. 151.
9. Y. Naitoh and R. Eckert, in *Cilia and Flagella*, M. A. Sleight, Ed. (Academic Press, New York, 1974), p. 305; Y. Satow and C. Kung, *J. Exp. Biol.*, in press; P. Brehm and R. Eckert, *Abstracts of the 8th Annual Meeting of the Society for Neuroscience* (1978), vol. 4, p. 234.
10. A. L. Hodgkin and A. F. Huxley, *J. Physiol. (London)* **116**, 497 (1952).
11. Y. Naitoh and R. Eckert, *Z. Vgl. Physiol.* **61**, 427 (1968).
12. C. M. Armstrong and L. Binstock, *J. Gen. Physiol.* **48**, 859 (1965); F. Bezanilla and C. M. Armstrong, *ibid.* **60**, 588 (1972).
13. P. Brehm, K. Dunlap, R. Eckert, *J. Physiol. (London)* **274**, 639 (1978).
14. S. Hagiwara and S. Nakajima, *J. Gen. Physiol.* **49**, 807 (1966).
15. P. G. Kostyuk and O. A. Krishtal, *J. Physiol. (London)* **270**, 545 (1977); K. S. Lee, N. Akaïke, A. R. Brown, *J. Gen. Physiol.* **71**, 489 (1978).
16. K. Takahashi and M. Yoshii, *J. Physiol. (London)* **279**, 519 (1978).
17. H. Machemer and R. Eckert, *J. Comp. Physiol.* **104**, 247 (1975).
18. D. Tillotson, *Abstracts of the 8th Annual Meeting of the Society for Neuroscience* (1978), vol. 4, p. 239; in preparation.
19. We thank D. Tillotson for providing ideas throughout the project, S. Hagiwara for stimulating discussions and for criticism of the manuscript, W. Moody, M. Masuda, L. Byerly, and J. Umbach for helpful comments, and R. Rivera for technical assistance. Supported by NSF grant GNS 77-19161.

13 July 1978; revised 11 October 1978

Transient Synapses in the Embryonic Primate Spinal Cord

Abstract. *Electron microscopic and tritiated thymidine autoradiographic analysis of the embryonic spinal cord in the rhesus monkey reveals considerable rearrangement of cellular and synaptic relationships in the posterior (sensory) quadrant during early developmental stages. This remodeling involves the death of an entire population of neurons that received synapses from sensory afferent axons and the possible relocation of these afferents upon subsequently generated viable substantia gelatinosa neurons.*

The complex cellular organization and synaptic circuitry of the adult central nervous system is the end result of an enormous number of changes that occur during ontogenetic development (1). We now report that considerable reorganization of synapses occurs in relation to the genesis of transient neurons in the region of the prospective substantia gelatinosa Rolandi of the primate spinal cord. The substantia gelatinosa, a structure that plays a role in nociception (2), consists of a translucent mixture of neurons and fibers forming lamina II of Rexed in the dorsal horn of the spinal cord (3). Analy-

sis of the simplified spinal cord of early embryos has revealed new developmental mechanisms for elaborating the extremely complex synaptic relationships of this region.

Fifteen rhesus monkey fetuses in the first third of the 165-day gestational period were fixed either by immersion or by vascular perfusion with 1 percent glutaraldehyde and 1.25 percent paraformaldehyde. Transverse slices (0.3 mm) from the fetal cervical cord were embedded in Epon-Araldite. Thick (1- μ m) sections were stained with toluidine blue or with a modified Protargol-gold